C. Morterra, A. Zecchina and G. Costa (Editors), *Structure and Reactivity of Surfaces*

METAL SUPPORT INTERACTION

R. PRINS[1], J.H.A. MARTENS[2] and D.C. KONINGSBERGER[2]

[1] Technisch Chemisches Laboratorium, Eidgenössiche Technische Hochschule, CH-8092 Zürich

[2] Laboratory of Inorganic Chemistry and Catalysis, Eindhoven University of Technology, NL-5600 MB Eindhoven

ABSTRACT

A Rh K EXAFS study showed that the rhodium particles in a Rh/Ta_2O_5 catalyst were fully reduced and in the 'normal' state after reduction in H_2 at 523 K. The metal particles contained about 73 rhodium metal atoms and had a diameter of 17 Å. After reduction at 858 K the catalyst was in the SMSI state. In addition to a contribution from rhodium nearest neighbours, two contributions from neighbouring tantalum ions could be detected. The tantalum ions were located in the reduced supporting oxide directly underneath the rhodium metal particles and in tantalum oxide covering the rhodium metal particles. Neither alloy formation, nor the formation of pillboxes or raftlike structures was observed.

INTRODUCTION

In catalysis as well as in the field of composite materials the interaction between a metal and a metal oxide is of prime importance for the mechanical properties. Sintering of supported metal catalysts (1) and adhesion in metal-ceramic composites (2) are therefore extensively studied. In catalysis there is the further interest in the possible influence of the metal-support interaction on the catalytic properties of the metal atoms in the metal-gas interface. It has been pointed out that the interaction between the ions in the metal oxide and the metal atoms in the interface occurs via a special van der Waals interaction of the ion-induced dipole type (3). The interaction energy is of the r^{-4} type and not of the r^{-6} type as between neutral atoms. The magnitude of this metal-ion interaction therefore can be substantial. Still, the contributions of more distant ions and atoms in both lattices cannot be ignored and therefore lattice matching has been claimed to give stronger bonding (4).

In catalysis it has been suggested that special metal cations may contribute to the sintering resistance of metal particles.

Thus Yermakov suggested that low valent metal cations of Mo, W, Ge and Co have a strong interaction with group VIII noble metal atoms and that these metal cations function as 'anchoring' sites for the noble metal particles (5). Analogously, Gallezot suggested that sintering of metal particles inside zeolites was prevented by transition metal cations which were exchanged into the zeolite (6). He also claimed that, because of the interaction between the metal particle and this transition metal cation, the metal particle became electron deficient. Recent work by Sachtler c.s. has confirmed the stabilizing influence of Fe^{2+} and Cr^{3+} cations in Pt/NaY zeolite (7). Huizinga and Prins extended the model of Yermakov by proposing that also cations of the noble metal proper could act as anchoring sites (8). They reported that the presence of Pt^{+} ions makes the Pt particles in Pt/Al_2O_3 more stable against sintering. In agreement with this, Anderson et al. calculated that the bonding between the O^{2-} anions and an oxidized Pt surface in an $Al^{3+}O^{2-}Pt^{+}Pt$ interface is strong (9).

A question which may be posed is, what makes the interaction between a metal particle and a transition metal ion different from that between a metal particle and a non-transition metal ion? For metal cations of the metal proper one may furthermore wonder why such metal cations do not become reduced.

In the classic ion-induced dipole interaction there is no principal difference between a transition metal ion and a non transition metal ion: $E=-q^2\alpha/2r^4$, in which q is the charge on the ion, α is the polarizability of the metal atom and r is the ion-atom distance. A lower valency of the metal cation even has an adverse effect on the interaction energy. Quantum mechanically, however, a lower valency of the transition metal cation leads to a smaller energy gap between the highest occupied orbitals (HOMO's) of the metal ion in the support surface and the lowest unoccupied orbitals (LUMO's) of the metal atom. Together with an increased size of the lower valent transition metal orbitals, this will give a larger interaction. Not enough theoretical MO results are available, however, to be able to fully test these qualitative predictions. Indeed, MO calculations have indicated that a bonding between a small metal cluster and a transition-metal oxide molecule can exist (10). But also the bonding between a Pt cluster and $Al_xO_y^{n-}$ clusters representing a Al_2O_3 fragment were found to be substantial (9). The interaction in the Pt/Al_2O_3 interface was calculated to be stronger with Al^{3+} cations than

with O^{2-} anions in the interface. One comes to the same conclusion on the basis of the induced-ion dipole formula $E=-q^2\alpha/2r^4$, which indicates that highly charged, small ions will have the largest interaction with a metal-atom. Cations like Al^{3+}, and O^{2-} anions rather than OH^- anions will therefore form relatively strong bonds. This suggests that the metal-support bonding might be increased by the creation of vacancies at the support surface and filling them with metal atoms. In that way metal cations in the support surface come in direct contact with metal atoms.

Since the discovery of the phenomenon of Strong Metal-Support Interaction (SMSI) a lot of research has been devoted to its explanation (11-13). SMSI can be defined as follows. After reduction at low temperatures (below 400 °C say) the adsorption capacities of metal particles supported on certain transition metal oxide supports is normal, whereas after a high temperature reduction (above 450 °C) the adsorption capacity for H_2 and CO has diminished drastically, although the metal particle size remains unaffected. This change in adsorption capacity is reversible, after oxidation and re-reduction at low temperature the adsorption capacity is normal. This Strong Metal-Support Interaction has similarities with the metal-support interaction discussed in the foregoing. The transition metal oxides which are used as a support are all reducable at higher temperature and this led to the suggestion that there might be a special (strong) interaction between the reduced transition metal ions and the metal atoms in the metal-support interface, hence the name SMSI. In an Xα-SW-MO calculation Horsley showed that there indeed is bonding between a Pt atom and a TiO_5^{7-} cluster (14).

Whatever the explanation of the metal-support interaction, it is clear that it is important to know the structure of the metal-support interface on an atomic scale. For that reason we started some years ago to use the Extended X-ray Absorption Fine Structure (EXAFS) technique in our study of the metal-support interface (3). But although the EXAFS-technique can very well measure the number and art of atoms or ions around a certain atom, it has the disadvantage of being a bulk technique. Therefore, in order to obtain meaningful results about the local structure of the metal atoms at the metal-support interface, we had to study very well dispersed metal particles and even then had to take care in obtaining good signal-to-noise data and to

use an analysis programme suited for reliably separating small signals of the interface metal atom from large signals of the other metal atoms (15). In this way we succeeded in observing for the first time the metal-oxygen anion contacts at the metal-support interface (3). Subsequent EXAFS studies on Rh, Pt and Ir on Al_2O_3, TiO_2 and MgO catalysts demonstrated that in all cases the metal particles had a three-dimensional rather than a two-dimensional shape (16-23). A raftlike structure was observed only in one very special case, in which a Ir/Al_2O_3 catalyst was prepared from $Ir_4(CO)_{12}/Al_2O_3$ (23). This catalyst proved to contain a carbon overlayer, which apparently determined the raftlike shape.

Although no $M\text{-}Al^{3+}$ distances have been observed thus far in M/Al_2O_3 catalysts, we have been able to measure $Rh\text{-}Ti^{n+}$ distances in Rh/TiO_2 (18, 19). With this and additional Rh-Rh and $Rh\text{-}O^{2-}$ information it proved possible to obtain a detailed picture of the metal-support interface of the Rh/TiO_2 catalyst in the normal, as well as in the SMSI state. In the SMSI state the metal particles were found to rest on reduced titania and a model was proposed as shown in Fig. 1. No indications for alloy formation were found (which is one of the proposed explanations for SMSI). Covering of the Rh particles by TiO_x fragments (which is another explanation) could not be fully excluded, however, and it was argued that if covering was occurring, it had to be very loose with irregular $Rh\text{-}TiO_x$ contacts. In full agreement with this suggestion Logan et al. recently observed in high resolution transmission electron microscopy pictures that the whole surface of a Rh/TiO_2 catalyst, the metal as well as the support, was covered with an amorphous layer of (probably reduced) TiO_2 after high temperature reduction (24).

A few problems remained from our EXAFS study on Rh/TiO_2, however. The first was that it could be argued that our reduction treatment of the Rh/TiO_2 catalyst was not severe enough and that therefore the covering was not tight and not observable by EXAFS. Secondly, although we did observe $Rh\text{-}Ti^{n+}$ distances of 3.4 and 4.3 Å, we did not observe the Ti^{n+} ions at 2 Å directly underneath the Rh atoms, as indicated in Fig. 1. On the other hand, the number of such Ti^{n+} neighbours is relatively small and combined with the low backscattering amplitude for Ti, the contribution of the 2 Å $Rh\text{-}Ti^{n+}$ distances might be too low for a reliable analysis. Thirdly, although we did not observe Rh-Ti

distances as in Rh-Ti alloys, others have claimed to have observed alloy distances in Rh/TiO_2 (25) and in Ni/Nb_2O_5 and Ni/TiO_2 (26).

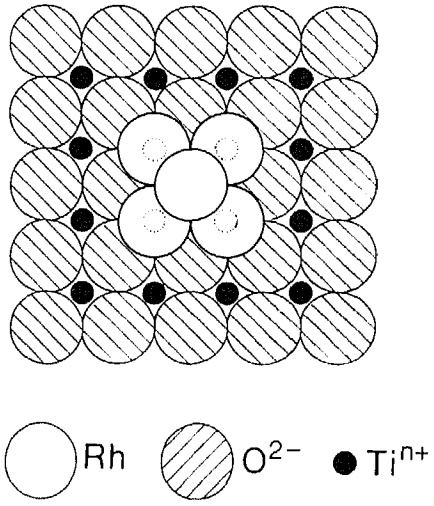

Figure 1 Model of the metal-support interface in a Rh/TiO_2 catalyst in the SMSI state

For these reasons we decided to extend our EXAFS studies of the metal-support interface of SMSI systems to the Rh/Ta_2O_5 catalyst. Ta_2O_5 is known to show SMSI behaviour (12) and, more importantly, Ta has a backscattering amplitude at high k-values which is 2 to 4 times larger than that of Ti (27). If Ta^{n+} ions are present underneath Rh interface atoms in the SMSI state or, alternatively, if Rh-Ta alloy distances are present, one must expect that such distances can be detected by EXAFS.

EXPERIMENTAL

A high surface area Ta_2O_5 support was prepared by adding a solution of 20 g $TaCl_5$ in 100 ml concentrated HCl to a mixture of 4 l distilled water and ice, which was acidified with HCl to pH=0. Approximately 300 ml of a NH_4OH solution was subsequently added dropwise to the $TaCl_5$ solution during a period of 100 min while vigorously stirring the solution. At the end of the ammonia addition the pH had increased to 6.0. After stirring for another 100 min, the precipitated $Ta(OH)_5$ was filtered off and washed several times with distilled water, thereafter it was carefully dried at 393 K for 24 h (heating rate 2 K min^{-1}), cooled down to

room temperature, powdered, dried again as described above, and finally calcined for 1 hr at 873 K (heating rate 2 K min^{-1}). The resulting 7 g Ta_2O_5 had a surface area of approximately 100 m^2g^{-1}

A 3 wt% Rh/Ta_2O_5 catalyst was prepared using the urea method (28). Three gram of the Ta_2O_5 was added to 350 ml distilled water at 365 K and the stirred solution was acidified with 8 N HCl to pH=2.5. Then 0.53 g of urea (a tenfold excess based on the amount of $RhCl_3$) was added and finally 0.23 g of $RhCl_3.3H_2O$ was added. Because of the slow decomposition of urea at 365 K, the pH of the solution increased very slowly. At a pH value of approximately 4, $Rh(OH)_3$ started to precipitate. After 10 h the catalyst precursor was filtered off and dried as described above for the Ta_2O_5 support. To remove the remaining urea the sample was calcined at 923 K, pre-reduced in hydrogen at 773 K and finally oxidized at 573 K. This sample was stored for further use. Temperature programmed reduction experiments indicated that reduction was complete at 470 K when using 4% H_2 in N_2. Hydrogen chemisorption measurements after reduction at 523, 773 and 873 K gave H/Rh values of 0.93, 0.14 and 0.06, respectively.

The stored Rh/Ta_2O_5 catalyst was pressed into a thin self supporting wafer, whose thickness was such that $\mu x=2.5$ at the rhodium K-edge, assuring an optimum signal-to-noise ratio in the rhodium EXAFS spectra. The wafer was mounted in an EXAFS cell which enabled in situ pretreatments in different gas atmospheres at temperatures ranging from 100 to 873 K. The sample, once mounted in the cell, was reduced in 100 % H_2 at 523 K for 1 h (heating rate 5 K min^{-1}). After cooling with liquid nitrogen to 100 K an EXAFS spectrum was recorded with the sample still under H_2. Thereafter, the sample was reduced in H_2 at 858 K for 15 min (heating rate 5 K min^{-1}), cooled down to 100 K and a second EXAFS spectrum was recorded. The EXAFS spectra of the reference compounds, rhodium foil, Rh_2O_3, $RhCl_3$, Rh_3Ta alloy, Ta powder and $TaCl_5$, were recorded at 100 K as well. The absorption spectra were recorded at the synchrotron radiation source (SRS) in Daresbury, U.K. The ring was operated at 2.0 GeV and with ring currents between 100 and 300 mA.

RESULTS

The backscattering amplitudes F(k) and the phase shift functions $\phi(k)$ which are necessary for analyzing the EXAFS data have been obtained from the reference compounds Rh_2O_3 (for the

Rh-O contributions), $RhCl_3$ (for the Rh-Cl contributions) Ta powder (for the Ta-Ta contributions) and $TaCl_5$ (for Ta-Cl contributions). In Table 1 all the relevant information concerning the references is given. The crystallographic data were taken from (29).

TABLE 1 Crystallographic data and Fourier transform ranges for the reference compounds

Compound	Edge	NN[a]	R[b]	N[c]	Fourier transformation n[d]	k-range	r-range
Rh foil	Rh	Rh	2.687	12	3	2.90-25.48	1.80-2.90
Rh_2O_3	Rh	O	2.05	6	3	2.64-22.17	0.68-2.12
$RhCl_3$	Rh	Cl	2.31	6	1	3.00-20.15	0.00-2.33
Ta	Ta	Ta	2.863	8	3	2.95-16.97	2.14-3.48
$TaCl_5$	Ta	Cl	2.37	6	3	2.44-15.87	0.18-1.88

a: Nearest Neighbour, b: Coordination Distance (Å), c: Coordination Number, d: Weighting factor in the Fourier transformation

F(k) and $\phi(k)$ for the Rh-Ta contributions could not be extracted from the the Rh_3Ta alloy, because the Rh-Rh and Rh-Ta peaks overlapped almost completely in the Fourier transform of the EXAFS spectrum of the alloy. Since the backscattering amplitude is only a function of the scattering atom (27) we took $F_{Ta-Ta}(k)$ from the L_{III} EXAFS spectrum of tantalum powder to represent $F_{Rh-Ta}(k)$. Because of the additivity of the contributions of the absorbing and scattering atoms, a phase shift function can be written as a linear combination of three other phase shift functions (27, 30). For $\phi_{Rh-Ta}(k)$ this leads to: $\phi_{Rh-Ta}(k) = \phi_{Rh-Cl}(k) + \phi_{Ta-Ta}(k) - \phi_{Ta-Cl}(k)$. Therefore we measured the Rh K-edge EXAFS spectrum of $RhCl_3$ and the Ta L_{III} EXAFS spectra of Ta powder and of $TaCl_5$. From these EXAFS functions we extracted $\phi_{Rh-Cl}(k)$, $\phi_{Ta-Ta}(k)$, and $\phi_{Ta-Cl}(k)$, and a linear combination of these three functions yielded the desired phase shift function for the Rh-Ta contributions.

Our procedure of analyzing the EXAFS spectra has already been described extensively in the literature (15, 16, 19). EXAFS spectra containing one or more shells are calculated by using the backscattering amplitudes F(k) and the phase shift functions $\phi(k)$ of suitable reference compounds. By varying the coordination number N, the coordination distance R, the Debye Waller factor

$\Delta\sigma^2$, and E_0, the correction on the edge position, one tries to fit the calculated EXAFS spectra to the measured spectra as accurately as possible. In two previous studies (18, 19) we described a recurrent optimization process for the separate analysis of the contributions from high-Z and low-Z scattering neighbours. Since in this study the contribution of the low-Z scatterer (oxygen) turned out to be very small and the remaining contributions originated from high-Z scatterers (rhodium and tantalum), this procedure could not be used. Moreover, the Rh-Rh and Rh-Ta contributions overlapped in the Fourier transform (cf. Figure 3f), making it impossible to use the difference file technique (15, 19). Therefore a single step multiple shell analysis with four parameters (N, R, $\Delta\sigma^2$ and E_0) for each shell was used. We calculated a Rh-Rh EXAFS function and two Rh-Ta EXAFS functions, added them, Fourier transformed the resulting spectrum and compared the result with the Fourier transform of the measured data. Because of the high-Z character of the main contributions (Rh and Ta), the use of k^3-weighted Fourier transforms was essential. Differences between the two spectra were minimized by varying the Rh-Rh and Rh-Ta parameters. The results of this analysis procedure are presented in Table 2.

TABLE 2 Final results from EXAFS data analysis

Treatment	NN	Coordination number	(a)	Distance (Å)	(a)	$\Delta\sigma^2$ (10^{-3} Å^{-2})	(a)	E_0 (eV)	(a)
R523	Rh	7.9	0.2	2.658	0.005	7.4	1	5.5	1
R858	Rh	7.9	0.2	2.650	0.005	7.0	1	7.8	1
	Ta	1.6	0.5	1.7	0.3	5.4	2	-10	3
	Ta	0.8	0.2	2.0	0.1	5.4	2	- 6	3

R : Reduction in H_2 at 523 or 858 K.
a : Estimated overall (experimental + systematic) error.

In Figure 2a, the raw EXAFS data for the sample reduced in pure H_2 at 523 K during 1 h and the calculated best fitting Rh-Rh EXAFS function are shown. The imaginary parts of the Fourier transforms of these EXAFS functions are shown in Figure 2b and their magnitudes in Figure 2c. Only minor contributions are present next to the Rh-Rh contribution.

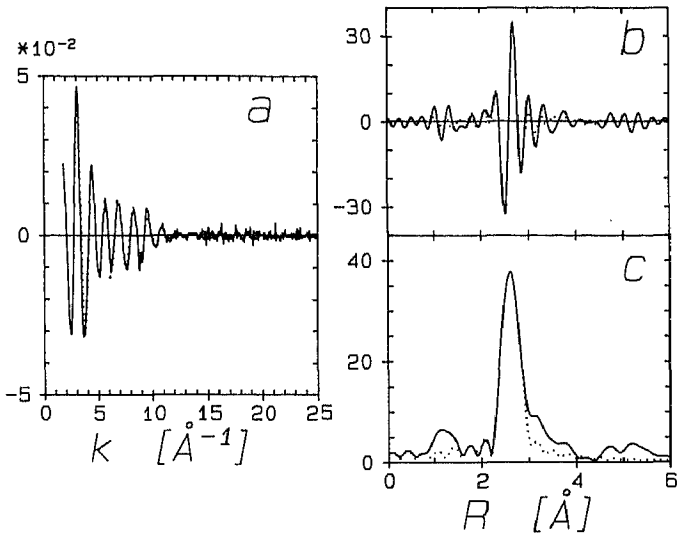

Figure 2 Rh/Ta_2O_5 after reduction at 523 K :
(a) Raw data (solid) and calculated Rh-Rh EXAFS (dotted line).
(b) Imaginary parts of the k^3-weighted Fourier transforms of the raw data (solid) and calculated Rh-Rh EXAFS (dotted line).
(c) Magnitudes of the k^3-weighted Fourier transforms of the raw data (solid line) and calculated Rh-Rh EXAFS (dotted line).

In Figure 3a the raw EXAFS spectrum and the calculated best fitting Rh-Rh EXAFS functions for the samples after a subsequent reduction at 858 K for 15 min are shown. In Figure 3b the imaginary parts of the k^3-weighted Fourier transforms of the measured data and calculated Rh-Rh EXAFS function are shown. Figure 3c shows the magnitudes of these Fourier transforms. The differences in Figures 3b and 3c at the left hand side of the main Rh-Rh peak are due to neighbouring tantalum ions. We tried to fit these differences with rhodium and oxygen neighbours as well, but the fits resulted in physically irrelevant parameters: coordination distances of about 1 Å for Rh-Rh and coordination numbers higher than 10 for oxygen. In addition, the resulting fit was worse than the fit with tantalum neighbours. Figures 3d, e and f show the raw data and the calculated best fitting Rh-(Rh+Ta) EXAFS functions, the imaginary parts of their k^3-weighted Fourier transforms and the magnitudes of the Fourier

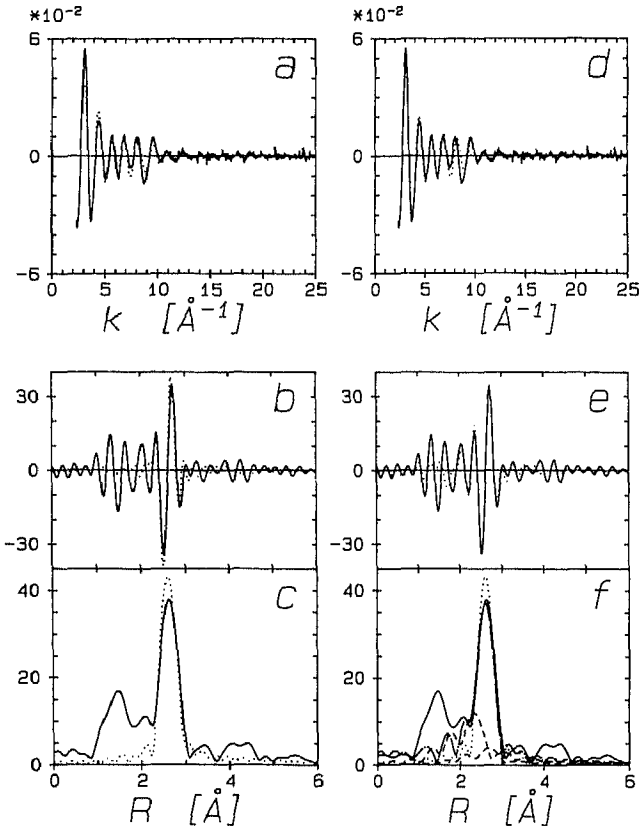

Figure 3 Rh/Ta_2O_5 after reduction at 858 K :
(a) Raw data (solid) and calculated Rh-Rh EXAFS (dotted line).
(b) Imaginary parts of the k^3-eighted Fourier transforms of the raw data (solid) and calculated Rh-Rh EXAFS (dotted line).
(c) Magnitudes of the k^3-weighted Fourier transforms of the raw data (solid line) and calculated Rh-Rh EXAFS (dotted line).
(d) Raw data (solid) and calculated Rh-(Rh+Ta) EXAFS (dotted).
(e) Imaginary parts of the k^3-weighted Fourier transforms of the raw data (solid) and calculated Rh-(Rh+Ta) EXAFS (dotted).
(f) Magnitudes of the k^3-weighted Fourier transforms of the raw data (solid), calculated Rh-Rh EXAFS function (dotted), the calculated Rh-Ta EXAFS functions (dashed) and the sum of the calculated Rh-Rh and Rh-Ta contributions (dash-dotted).

transforms of the raw data and of the three separate contributions. Clearly, the agreement at the left hand side of the main Rh-Rh peak in the Fourier transform is better. The Fourier transforms of the EXAFS spectra were complicated by the k-dependence of F(k) and $\emptyset$(k). Therefore, the transforms were corrected for F(k) and $\emptyset$(k) from rhodium foil, the reference for the Rh-Rh contribution, which was the major contribution in all spectra. As a result, in the Fourier transforms the Rh-Rh contributions 'peaked' at the correct Rh-Rh distance and the imaginary parts of the Fourier transforms were more or less symmetric (15). But the peaks corresponding to other minor contributions shifted to seemingly longer or shorter distances and were asymmetric. However, since the same correction has been applied to measured and calculated data, the calculated coordination numbers and distances represented those in the sample as accurately as possible.

DISCUSSION

Rh/Ta_2O_5 after Reduction at 523 K

According to the TPR experiments, reduction of the sample should be complete at 523 K. A careful analysis of the EXAFS spectrum confirmed this. Figure 2 shows that the main peak is due to a Rh-Rh contribution. The other peaks in Figure 2b and c are very small; the shoulder at the right hand side of the main peak could not be fitted with a Rh-Rh, a Rh-O or a Rh-Ta contribution. The peak around 1.2 Å in Figure 2c is due to an artefact that will be discussed in the following.

From Table 2 it can be concluded that on the average each rhodium atom had approximately 7.9 rhodium neighbours at 2.658 Å, which is slightly shorter than the Rh-Rh bulk distance (2.687 Å). Using the calibration procedure as described in (21), we estimated from the Rh-Rh coordination number that the particles were approximately 17 Å in diameter and contained about 73 ± 5 rhodium atoms. The H/Rh value should be about 0.95 according to an experimental calibration method as well as a computer model calculation (21). This agrees excellently with the measured value, H/Rh = 0.93, and demonstrates that the metal particles were in the 'normal' state.

In the EXAFS spectra of fully reduced supported metal catalysts, a metal-oxygen contribution from the metal atoms in the metal-support interface having oxygen neighbours has

frequently been reported (15, 17, 19, 22). In the Fourier transform, such a contribution is situated at the left hand side of the main Rh-Rh peak. Since the relative extent of the metal-support interface decreases with increasing particle size, the contribution from neighbouring oxygen ions decreases with increasing particle size as well (15, 17). For a 73 atom metal particle about 30 % of the rhodium atoms are situated in the metal-support interface. When these rhodium atoms each have 2 to 3 oxygen neighbours, the average Rh-O^{2-} coordination number is about 0.6 to 0.9 and, because of the low coordination number and the low backscattering amplitude of oxygen, the corresponding contribution in the Fourier transform should be smaller by more than an order of magnitude compared to the Rh-Rh contribution. Therefore, no contribution from neighbouring oxygen ions could be detected in the EXAFS spectrum of the sample reduced at 523 K.

Rh/Ta_2O_5 after Reduction at 858 K

After reduction at 773 K, the H/Rh value determined with hydrogen chemisorption decreased to 0.14, and after reduction at 873 K to 0.06. Clearly, after reduction at 858 K the metal particles were in the SMSI state. Since the Rh-Rh coordination number remained unchanged (cf. Table 2) the basic structure of the metal particles was still the same. In a study of Pt/TiO_2 it was shown that in the SMSI state the Pt particles are spread over the support and that 'pillboxes' are formed (31). If such a spread of the metal particles had also occurred in Rh/Ta_2O_5, it should have been accompanied by a significant decrease in the Rh-Rh coordination number. We did not observe such a decrease and therefore we conclude that in the case of Rh/Ta_2O_5 spreading of the rhodium particles did not occur. This is in agreement with literature data, which indicate that rhodium does not 'wet' TiO_x surfaces (24), like Pt does (31).

Another explanation was the formation of alloys (11). We did not observe contributions from neighbouring tantalum atoms at distances in the range of 2.7-2.8 Å (in the Rh_3Ta bulk alloy, the Rh-Ta distance is 2.729 Å (29)). Therefore, alloy formation can be ruled out in our Rh/Ta_2O_5 catalyst. In three other EXAFS studies the observation of an alloy in the SMSI state has been claimed (25, 26, 32). However, we think that the presence of the carbon support might have greatly influenced PtTi alloy formation in the system Pt-TiO_2/C (32), while the assignment of a peak in

the EXAFS spectrum of Rh/TiO_2 to a Rh-Ti alloy contribution (25) is highly questionable because of the applied analysis procedure (19). The claim of Ni-Nb and Ni-Ti alloy contributions in the EXAFS spectra of Ni/Nb_2O_5 and Ni/TiO_2 (26), respectively, seems even more questionable because of the extremely narrow window used in the reverse Fourier transformation and because of the fact that others have found that a large fraction of the Ni ions in such systems is not reduced at all, but forms a Ni-Ti-O compound (33). In our opinion therefore, no unequivocal EXAFS proof for the existence of an alloyed phase in the SMSI state of a M/TiO_2 (or related) system has been presented yet.

Table 2 shows that the Rh-Rh coordination distance decreased by 0.008 Å when the reduction temperature was increased. This is only a small change for a metal particle which contracts, because it is no longer covered with adsorbed hydrogen in the SMSI state. A decrease of 0.05 Å was reported for very small rhodium metal particles in Rh/TiO_2 (19). The difference between the Rh/Ta_2O_5 and Rh/TiO_2 catalysts must be due to the fact that the metal contraction is largest in the surface layer (34). Small metal particles will therefore show a larger decrease in the average Rh-Rh distance than bigger metal particles.

In the EXAFS spectrum of the sample after reduction at high temperature, two more contributions were present which both originated from tantalum neighbours at notably short distances. In the Fourier transforms, the peaks from both Rh-Ta contributions overlapped to a large extent with the much larger Rh-Rh contribution. As a result, the uncertainty in the Rh-Ta coordination number is larger than the uncertainty in the Rh-Rh coordination number. The estimated uncertainty in the 2.0 Å Rh-Ta coordination number is about 0.2 and in the distance about 0.1 Å. The uncertainty in the 1.7 Å Rh-Ta contribution is somewhat larger than that in the 2.0 Å Rh-Ta contribution, because of an irregularity around $k = 9$ $Å^{-1}$ in the EXAFS spectra of the Rh/Ta_2O_5 sample reduced at 858 K (see Figure 3a). This irregularity gave rise to a peak in the Fourier transform at $r = 1.6$ Å. In the Fourier transforms of the sample reduced at 523 K (see Figure 2b and c), the contribution from this artefact was small, clearly separated from the Rh-Rh peak and caused only small deviations in the Fourier transform. The 1.7 Å Rh-Ta contribution had a main peak at 2.3-2.4 Å in the Fourier transform and two sidelobes at 1.8 and 1.4 Å (see Figure 3f). The

main peak is shifted from the real Rh-Ta distance because the Fourier transform was corrected for Rh-Rh phase shift and backscattering amplitude. The two sidelobes interfered with the artefact at 1.6 Å and thus, only the main peak of this contribution could be used to determine the accompanying parameters. This caused an additional uncertainty in the parameters for the 1.7 Å Rh-Ta contribution: about 0.2 in the Rh-Ta coordination number and approximately 0.1 Å in the Rh-Ta coordination distance (additional to the uncertainty in the 2.0 Å Rh-Ta contribution). In the Rh-Ta distances, another uncertainty has to be considered. The phase shift function for this absorber-scatterer pair has been composed from three phase shift functions. Hence, the resulting uncertainty in the final phase shift function was the sum of the uncertainties in the three individual phase shift functions. We estimated that based on this, the uncertainty in the resulting calculated Rh-Ta distances was about 0.1 Å. In Table 2, the final uncertainties of all parameters are summarized.

Because the irregularity around k = 9 $Å^{-1}$ created problems, we tried to eliminate it from the spectrum by subtracting the best fitting calculated spectrum from the measured data. The difference spectrum consisted mainly of this artefact. Using a Hanning window between 8 and 9.5 $Å^{-1}$, we isolated the artefact from the difference file and subtracted it from the measured data. The Fourier transform of the resulting spectrum was indeed better than the spectrum of the raw data, the artificial peak around r = 1.6 Å was almost completely removed. However, this procedure introduced new, smaller artefacts around 8 and 9.5 $Å^{-1}$ and it was impossible to completely remove the artefact without introducing new artefacts. Nevertheless, our conclusion is that the peak in the Fourier transform around r = 1.6 Å is indeed induced by the artefact around k = 8-9 $Å^{-1}$.

Although the overall uncertainty in the Rh-Ta parameters is quite large and made a detailed interpretation not very meaningful, there is no doubt that tantalum ions are present at distances between 1.4 and 2.1 Å. These are very short coordination distances and can arise only from Ta^{n+} ions in direct contact with rhodium atoms in the metal-tantalum (sub)oxide interface. These ions may be located directly underneath the rhodium metal particles. This indicates that indeed the Ta_2O_5 support under the metal particles had been

reduced. However, the coordination numbers of the Rh-Ta contributions are rather high. When only the rhodium atoms in the metal-support interface have Ta^{n+} neighbours, and the support does not expose a large amount of bare Ta^{n+} ions, these coordination numbers cannot exceed 0.3. For a 73 atom half spherical metal particle about 30 % of the metal atoms is in the metal-support interface and we assumed that each interfacial rhodium atom could have up to one tantalum neighbour at such a short distance. Therefore we conclude that also the surface rhodium atoms, which are not in the metal-support interface, must be in direct contact with Ta^{n+} ions and that the metal particles were substantially covered with reduced Ta_2O_5. The direct contact between rhodium atoms and tantalum ions after reduction at high temperature could result in a strong interaction between metal particle and support.

In (18, 19) we reported Rh-Ti^{n+} distances of 3.4 and 4.3 Å. Such longer distances have not been observed for the Rh/Ta_2O_5 catalyst in the SMSI state. The reason is the following. TiO_2 has a very simple and very regular structure. The 3.4 and 4.3 Å distances are therefore well separated from other distances. For supports with a more complicated crystal structure like Al_2O_3 and Ta_2O_5 this is unfortunately not the case. At short distances, the Rh-Ta^{n+} (or Rh-Al^{3+}) distances are well separated, but many Rh-Ta^{n+} distances can occur between 3 and 5 Å, each with a rather low coordination number. This makes makes it almost impossible to observe the longer Rh-Ta^{n+} distances and explains also why Rh-Al^{3+} distances have never been observed.

CONCLUSIONS

Apart from the Rh-Rh contribution, no other contributions could be detected in the EXAFS spectra of the Rh/Ta_2O_5 catalyst reduced at 523 K. From the Rh-Rh coordination number it was concluded that the particles were about 17 Å in diameter and contained about 70 to 80 rhodium atoms. After reduction at 858 K the sample was in the SMSI state. The Rh-Rh coordination number remained unchanged. Thus, the basic structure of the metal particles remained intact. Any spread of the metal particles over the support like a pillbox formation could be excluded. Alloy formation had not taken place either. In the SMSI state the rhodium atoms in the metal-support interface had tantalum ions as neighbours at very short distances, ranging from 1.4 to 2.1 Å.

This indicated that the Ta_2O_5 oxide directly underneath the metal particles was reduced to a lower oxide of Ta_2O_5. In addition, the metal particles were substantially covered with reduced Ta_2O_5.

In the Rh/TiO_2 samples we did not observe any covering, but we could not exclude partial covering either (19, 20). The fact that the rhodium metal particles in Rh/Ta_2O_5 are covered to a larger extent than the metal particles in Rh/TiO_2 can be explained in several ways. First of all, the metal particles in Rh/Ta_2O_5 are much larger than the metal particles in the Rh/TiO_2 samples (19, 20) and coverage has up to now only been reported in literature for larger metal particles. Another reason might be the fact that the Rh/Ta_2O_5 sample was reduced at much higher temperature (858 K) than the Rh/TiO_2 samples (673 and 723 K). A third reason may be found in the preparation method. The Rh/TiO_2 samples were prepared by exchanging with a solution of $Rh(NO_3)_3$ which had a relatively high pH. The Rh/Ta_2O_5 sample was prepared using the urea method and therefore, the starting pH was low. Thus, during the preparation of the Rh/Ta_2O_5 sample, some Ta_2O_5 might have dissolved and later precipitated on top of the rhodium metal particles. This kind of coverage has already been reported for Rh/V_2O_3 by van der Lee et al. (35) and for $Rh-V_2O_3/SiO_2$ by Kip et al. (36). After reduction at high temperature, this Ta_2O_5 on top of the metal particles will become reduced and may have an intimate contact with the metal particle, giving rise to $Rh-Ta^{n+}$ bonding.

ACKNOWLEDGEMENT

This study was supported by the Netherlands Foundation for Chemical Research (SON) with financial aid form from the Netherlands Organization for the Advancement of Pure Research (ZWO).

REFERENCES

1 P. Wynblatt and N.A. Gjostein, Progr. Solid State Chem., 9 (1975) 21.
2 J.T. Klomp, Proc. Brit. Ceram. Soc., (1984) 249.
3 J.B.A.D. van Zon, D.C. Koningsberger, H.F.J. van 't Blik, R. Prins and D.E. Sayers, J. Chem. Phys., 80 (1984) 3914.
4 C.A.M. Mulder and J.T. Klomp, J. Phys. (Paris), 46 (1985) C4-111.
5 Y.I. Yermakov, Catal. Rev.-Sci. Eng., 13 (1976) 77; Y.I. Yermakov and B.N. Kuznetsov, J. Mol. Catal., 9 (1980) 13.
6 P. Gallezot, Catal. Rev.-Sci. Eng., 20 (1979) 121.
7 M.S. Tzou, H.J. Jiang and W.M.H. Sachtler, Appl. Catal., 20 (1986) 231; ibid, 39 (1988) 255.
8 T. Huizinga and R. Prins, J. Phys. Chem., 87 (1983) 173.

9 A.B. Anderson, C. Ravimohan and S.P. Mehandru, Surf. Sci., 183 (1987) 438.
10 A.B. Anderson and M.K. Awad, Surf. Sci., 183 (1987) 289.
11 S.J. Tauster, S.C. Fung and R.L. Garten, J. Am. Chem. Soc., 100 (1978) 170.
12 S.J. Tauster and S.C. Fung, J. Catal., 55 (1978) 29.
13 S.J. Tauster, S.C. Fung, R.T.K. Baker and J.A. Horsley, Science, 211 (1981) 1121.
14 J.A. Horsley, J. Am. Chem. Soc., 101 (1979) 2870.
15 J.B.A.D. van Zon, D.C. Koningsberger, H.F.J. van 't Blik, D.E. Sayers, J. Chem. Phys., 82 (1985) 5742.
16 H.F.J. van 't Blik, J.B.A.D. van Zon, T. Huizinga, J.C. Vis, D.C. Koningsberger and R. Prins, J. Am. Chem. Soc., 107 (1985) 3139.
17 D.C. Koningsberger, J.B.A.D. van Zon, H.F.J. van 't Blik, G.J. Visser, R. Prins, A.N. Mansour, D.E. Sayers, D.R. Short and J.R. Katzer, J. Phys. Chem., 89 (1985) 4075.
18 D.C. Koningsberger, J.H.A. Martens, R. Prins, D.R. Short and D.E. Sayers, J. Phys. Chem., 90 (1986) 3047.
19 J.H.A. Martens, R. Prins, H. Zandbergen and D.C. Koningsberger, J. Phys. Chem., 92 (1988) 1903.
20 J.H.A. Martens, R. Prins and D.C. Koningsberger, J. Phys. Chem., in press.
21 B.J. Kip, F.B.M. Duivenvoorden, D.C. Koningsberger and R. Prins, J. Catal., 105 (1987) 26.
22 D.C. Koningsberger and D.E. Sayers, Solid State Ionics, 16 (1985) 23.
23 F.B.M. van Zon and D.C. Koningsberger, to be published.
24 A.D. Logan, E.J. Braunschweig, A.K. Datye and D.J. Smith, Langmuir, 4 (1988) 827.
25 S. Sakellson, M. McMillan and G.L. Haller, J. Phys. Chem., 90 (1986) 1733.
26 G. Sankar, S. Vasudevan and C.N.R. Rao, J. Phys. Chem., 92 (1988) 1878.
27 B.K. Teo and P.A. Lee, J. Am. Chem. Soc., 101 (1979) 2815.
28 J.W. Geus, in G. Poncelet, P. Grange and P.A. Jacobs (Eds.), Preparation of Catalysts III, Elsevier, Amsterdam, 1983, p.1
29 Rh metal: Wyckhoff Crystal Structures, 1 (1963) 10; Rh_2O_3: Struct. Rep., 40a (1976) 301; $RhCl_3$: Struct. Rep., 29 (1972) 275; Rh_3Ta: Struct. Rep., 29 (1972) 130; Ta metal: Wyckhoff Crystal Structures, 1 (1963) 16; $TaCl_5$: Struct. Rep., 22 (1968) 237.
30 J.H. Sinfelt, G.H. Via, F.W. Lytle and R.B. Greegor, J. Chem. Phys., 72 (1980) 4832.
31 R.T.K. Baker, E.B. Prestridge and R.L. Garten, J. Catal., 56 (1979) 390.
32 B.C. Beard and P.N. Ross, J. Phys. Chem., 90 (1986) 6811.
33 H.C. zur Loye and A.M. Stacey, J. Am. Chem. Soc., 107 (1985) 4567.
34 A.D. King and D.P. Woodruff, Eds., The Chemical Physics of Solid Surfaces and Heterogeneous Catalysis, Elsevier, Amsterdam, 1981.
35 G. van der Lee, B. Schuller, H. Post, T.L.F. Favre, V. Ponec, J. Catal., 98 (1986) 522.
36 B.J. Kip, P.A.T. Smeets, J. van Grondelle, and R. Prins, Appl. Catal., 33 (1987) 181.

Dr. D. Reinalda (Royal/Dutch-Shell Laboratory, Amsterdam, The Netherlands) **asked:**

Reduced TiO_2 is a semiconductor and by hopping electrons may move through the bulk. Yet, the reduced Ti ions do tend to creep over the Rh particles. What may be the driving force of this phenomenon?

Answer to the question of Dr. D. Reinalda

The formation of reduced TiO_2 on top of noble metal particles may take place through creeping of TiO_x from the TiO_2 surface onto the metal surface, or through reduction of TiO_2 fragments which were deposited on top of the metal particles during the wet impregnation step. The latter mechanism is well established (Ponec c.s., see for instance J. Catal., 98, 522, 1986), the former much less so. It is not clear what the driving force for this creep mechanism is, but it might have to do with metal bonding between the noble metal and Magnelli phase Ti_nO_{2n-1} material, which is a metallic conductor. A third possibility for the formation of reduced transition metal oxide on top of the noble metal particles is to first form a mixed metal oxide through calcination, and then to reduce this mixed metal oxide. In this way, Kip et al. formed V_2O_3 on top of Rh when $RhVO_4$ on SiO_2 (formed via calcination of $Rh(NO_3)_3$ and NH_4VO_4 on SiO_2) was reduced in flowing H_2 (Appl. Catal., 33, 157, 1987).